TUDelft

Delft University of Technology

NLPO analyses of three terraced houses with the SLaMA method
Module 3 – Harmonisatie berekeningsmethode

Tavus, A.; Messali, F.

Important note
To cite this publication, please use the final published version (if applicable).
Please check the document version above.

Module 3 – Harmonisatie berekeningsmethode

NLPO ANALYSES OF THREE TERRACED HOUSES WITH THE SLAMA METHOD

Authors: Ahmet Tavus, Francesco Messali

This document is made available via the website 'Structural Response to Earthquakes' and the TU Delft repository. While citing, please verify if there are recent updates of this research in the form of scientific papers.

Table of Contents

1 Introduction

This report summarizes the results of the nonlinear pushover (NLPO) analyses performed with the SLaMA method for three different terraced houses in support to the development of NPR 9998 Module 3.

The three analysed buildings are hereinafter referred as follows:
- Building B;
- Building C;
- Building D.

For the sake of simplicity, where the following text refers to an article, a section or an Annex "of NPR", this is in fact referring to NPR 9998 [1]. The spectra used for the site specific assessments are taken from the NEN webtool [2].

The NLPO analyses are performed in accordance to the SLaMA method as described in Section G of NPR.
The individual capacity of the elements is computed as described in sections G.9.2 for piers and G.9.3 for spandrels. The local acceptance criteria of NPR are considered to assess the performance of the building as described for piers in sections G.9.2.2 and G.9.2.3 for piers, and in section G.9.3.1 for spandrels.

A short description of the SLaMA procedure and of the assumptions made is given in section 2.

The terraced houses are evaluated without considering the soil-structure interaction (SSI) effects, and a fixed based analysis is performed.

2 SLaMA method and assumptions

The SLaMA analyses are performed according to the procedure and the equations recommended in Annex G of NPR.

Each analysis is based on the following steps and assumptions:

-   Each perforated wall (i.e. each façade or internal wall) is divided into single elements. The meshing procedure follows the recommendations reported in Section G.9.2.1 of NPR, based on the identification of the compressive struts in the walls (Figure 1a). An example of the mesh of a façade is presented in Figure 1b.
-   The roof (i.e. whatever lies above the attic level) is not modelled, but its mass is accounted for.
-   Only the inner leaves of the cavity walls are modelled.
-   RC floors are able to restrain the rotations at the top of the piers (i.e. the piers are assumed to be double clamped); timber floors are not. In the latter case, the piers are assumed to behave as cantilever elements unless the adjacent spandrels are strong enough to prevent the rotations. This condition occurs when the force acting on the spandrel needed to guarantee the equilibrium with force acting at failure at the top of the pier (assumed as double clamped) does not exceed the resistance of the spandrel.
-   The vertical loads acting on each pier and contributing to the structural stability are computed by considering the initial static configuration. For two-way spanning floors, the loads are distributed considering the tributary area of each pier. No load is transferred to non-loadbearing walls.
-   The possible contribution of the flanges is accounted for according to the method of Moon [3]. The flanges are assumed to be present only between loadbearing walls, for which the interlocking at corners is possible.
-   The contribution of the non-loadbearing walls is also included. However, since they have no overburden in the initial stage and they are assumed to be disconnected from the loadbearing walls, their force capacity is based on the self-weight only and it is therefore extremely limited.
-   The second order effects are taken into account for each pier as reported in Section 4.4.2.2 of NPR.
-   The capacity of each single perforated wall is evaluated separately for every storey. That is computed by summing up the capacity of the individual members at that level.
-   The capacity of the structure is then computed for the whole building at each storey level. When the floor is sufficiently stiff to provide a box-behaviour (i.e. if the piers are connected at top by a RC floor which is assumed to be able to redistribute the forces), the contributions of the different perforated walls are summed up. With timber floors, the capacity is computed separately for each perforated wall, and the minimum capacity in terms of normalized accelerations (see the next point) is considered.
-   The capacity is scaled by the effective mass of the sub-structure (for two-storey buildings, either the whole building or the top storey only). The capacity of the sub-systems is then presented in terms of accelerations and a comparison is made to identify the sub-structure whose failure is governing (i.e. reaches the lowest acceleration).
-   Both modal and mass proportional distribution of the lateral loads are considered. The masses are localised at the floor level.
-   For the modal distribution of the lateral loads, an approximated linear distribution is assumed for the sake of simplicity.
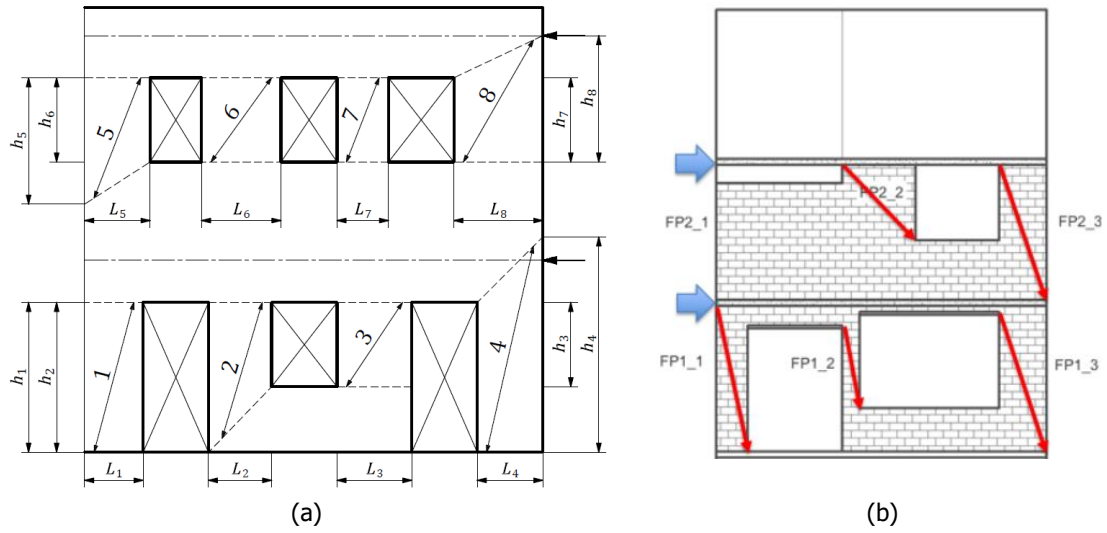
Figure 1. Graphical representation of the compressive struts of a perforated wall as recommended in [2] (a), and example of meshing of a façade (b).

3 Building B

Building B comprises of three two-storey building units, with three appendices and an extra one-storey building. The building units are connected one another only through the outer leaf of the cavity wall. Also the appendices are connected with the main building unit through the outer leaf of the cavity wall. Finally, the concrete slab is discontinuous between the individual units. No significant interaction is expected between the building units and between the building unit and the appendix. For this reason only one building unit is analysed.

The discretization of the two facades is shown in Figure 2 and Figure 3 for the positive and negative loading, respectively. The internal walls are all modelled as cantilever piers, not connected to any other wall. As mentioned in Section 2, the spandrels are not modelled due to the presence of a bidirectional RC slab which constrain the rotations at the top of the piers.

The effective mass computed for the building is 68.2 t, assuming the first mode shape as linear.
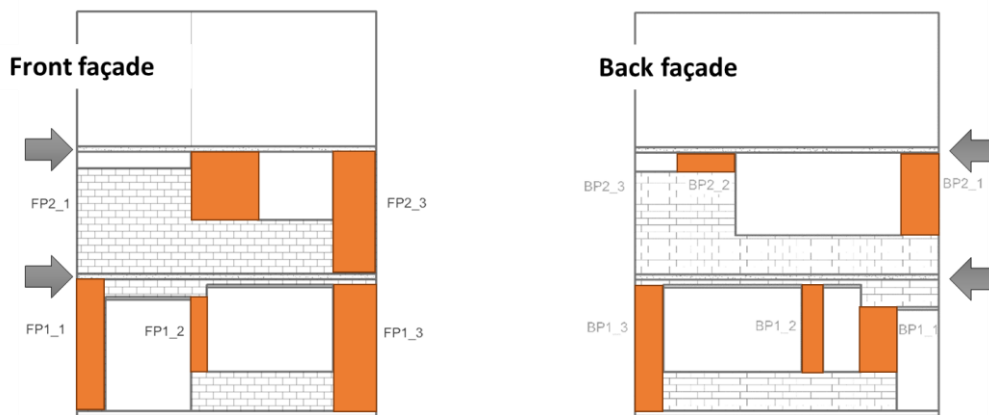

Figure 2. Piers defined on the front and back façades of Building B for positive loading.
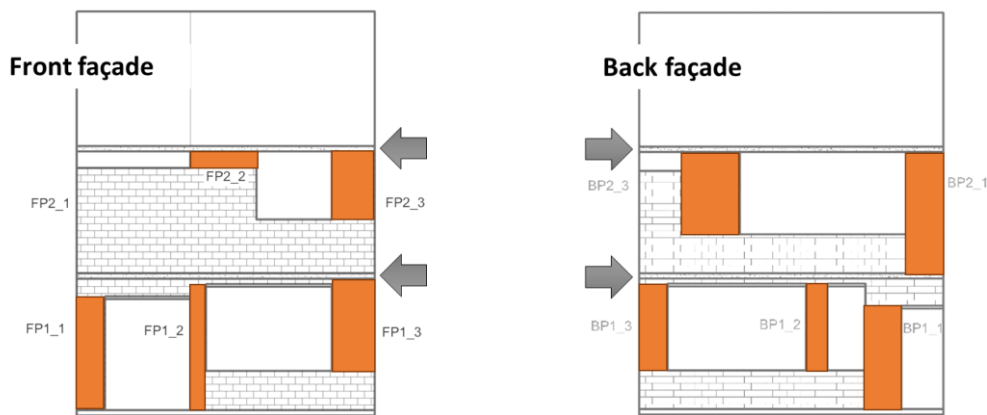
Figure 3. Piers defined on the front and back façades of Building B for negative loading.

3.1 Capacity of the structure

As described in section 2, a capacity curve is computed for each storey level and for both the mass-proportional and the mode-proportional lateral load distributions. The capacity curves obtained are shown in Figure 4 and Figure 5 for the positive and negative loading direction, respectively. In both cases, the capacity of the ground

storey level (in terms of normalized accelerations) is largely smaller than that of the first storey level. For this reason, a soft-storey mechanism at the ground-storey level is expected.

Besides, the mode-proportional distribution of the lateral loads is governing for both the directions.
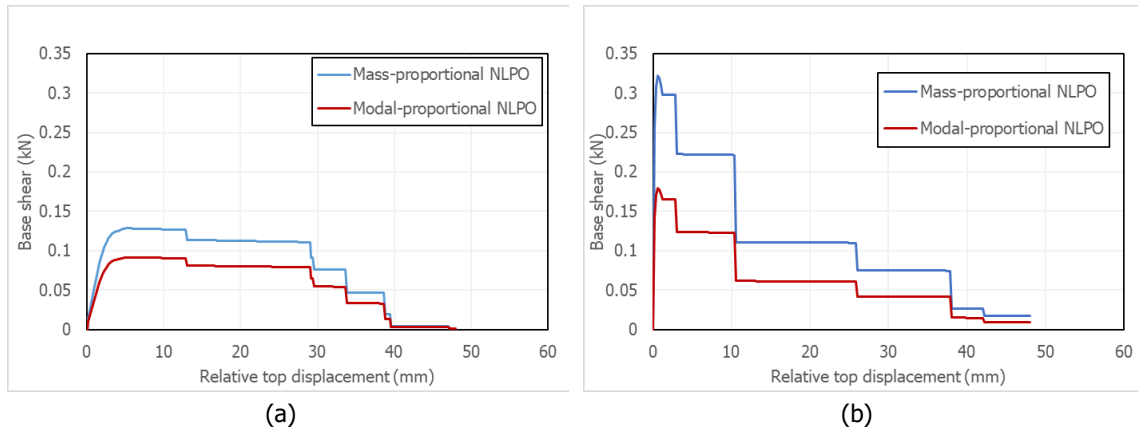

Figure 4. Capacity curve of the ground (a) and first (b) storey level for the positive loading direction.
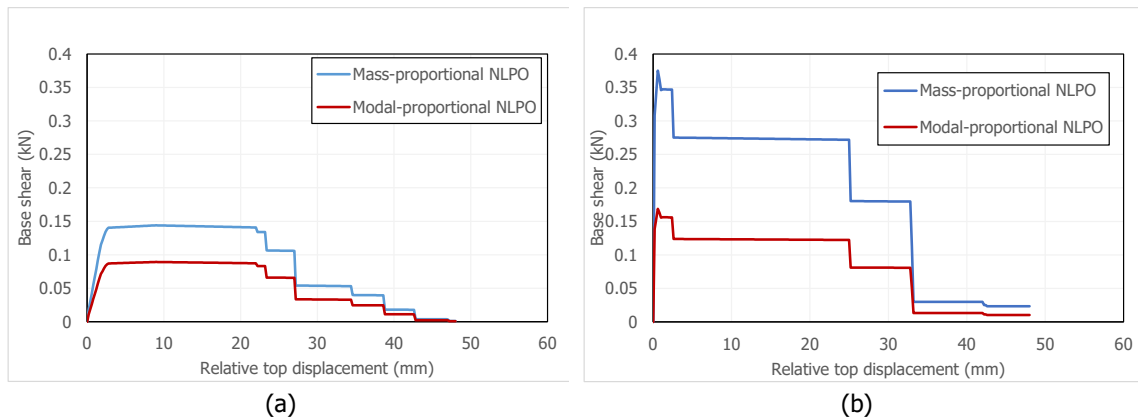

Figure 5. Capacity curve of the ground (a) and first (b) storey level for the negative loading direction.

The type of failure observed in each pier (either shear – as described in section G.9.2.2 of NPR9998 – or flexure – section G.9.2.3) is shown in Figure 6 and Figure 7 for positive and negative loading, respectively. The blue colour represents flexural failure and the green colour shear failure. Except the central pier of the first storey level on the back façade, which undergoes shear failure, flexure is governing for all the other piers. All the internal non-loadbearing walls undergo flexural failure. Especially, at the ground storey level (the governing storey, as described above), all the piers are characterized by flexural failure, so that the overall behaviour of the structure can be defined as 'ductile'. This is shown also by the equivalent bilinear curves derived for the structure and shown in Figure 8 (for the governing mode-proportional lateral load distribution). The relevant points of the curves are reported in Table 1.

The near collapse (NC) displacement is computed at the point corresponding to a 50% drop of the force capacity with respect to the peak load, since the sequence of failure of the piers does not show the complete failure of a façade before that the NC displacement is achieved, as shown in Figure 9 and Figure 10 for positive displacements and negative loading, respectively (it should be noted that the piers with a green number fail before the 50% drop, whereas those with a red number fail after that point).

The bilinear curve for negative displacements has a slightly larger capacity in terms of normalized acceleration, but a smaller displacement capacity. For this reason, the negative direction is the one considered for the assessment of the building.
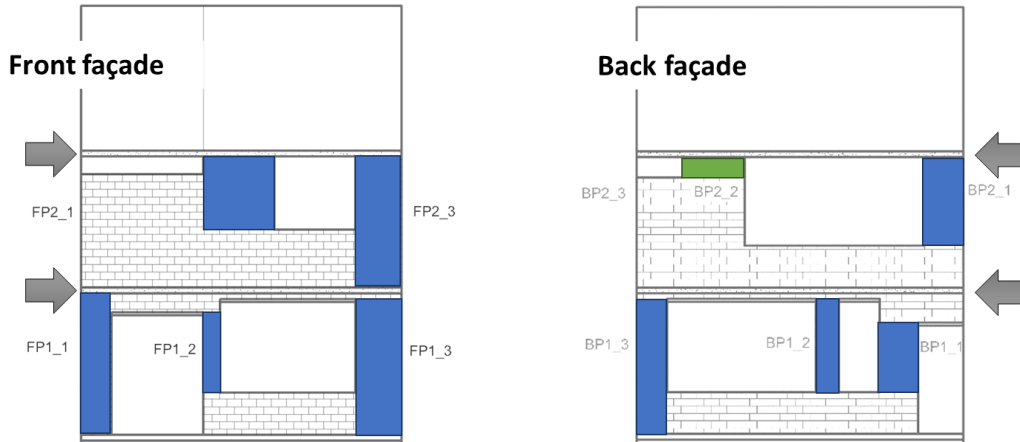
Figure 6. Failure of the piers of the front and back façades for positive loading. The blue colour represents a flexural failure and the green colour a shear failure.
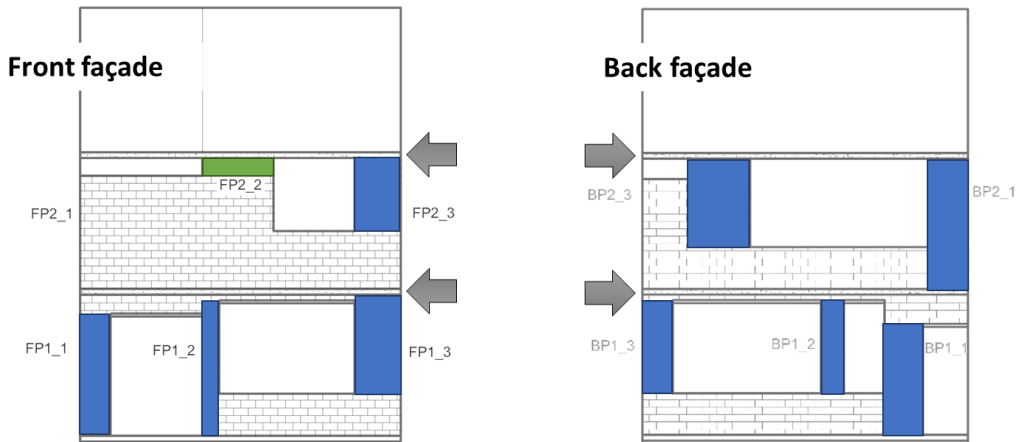

Figure 7. Failure of the piers of the front and back façades for negative loading. The blue colour represents a flexural failure and the green colour a shear failure.
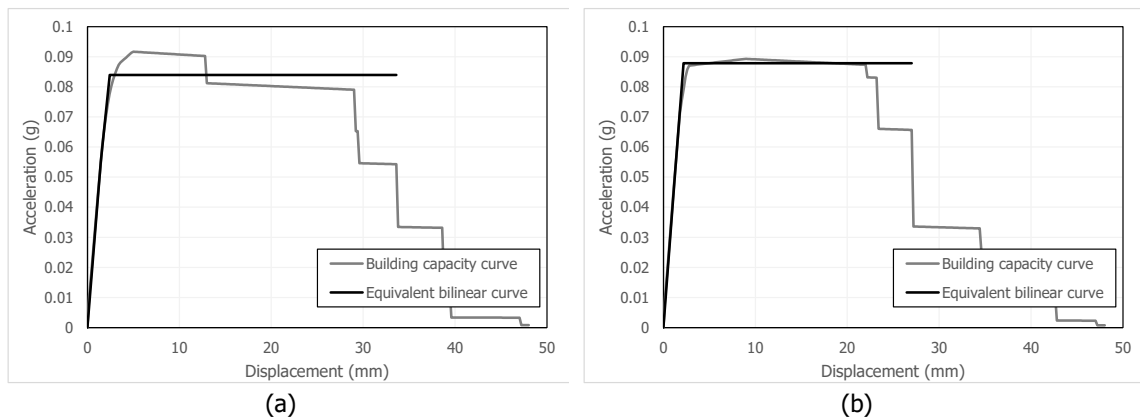

Figure 8. Equivalent bilinear capacity curve derived for the mode-proportional NLPO, for positive (a) and negative (b) loading direction.

Table 1. Relevant points of the equivalent bilinear curves.

	d_y (mm)	d_{NC} (mm)	a_{max} (g)
Positive loading	2.42	33.6	0.084
Negative loading	2.20	27.0	0.088

Figure 9. Sequence of NC collapse of the piers on the front and back façade for positive loading. The piers with a green number fail before the 50% drop, whereas those with a red number fail after that point.
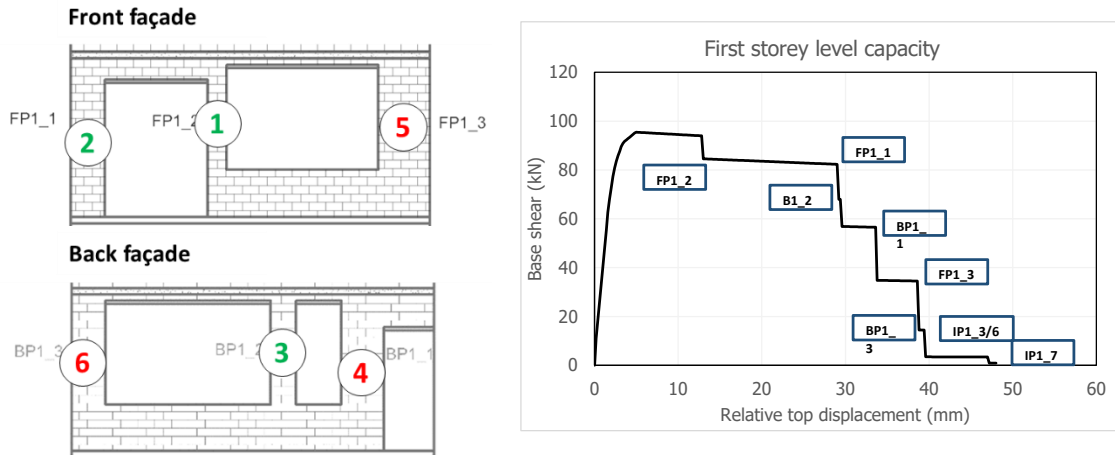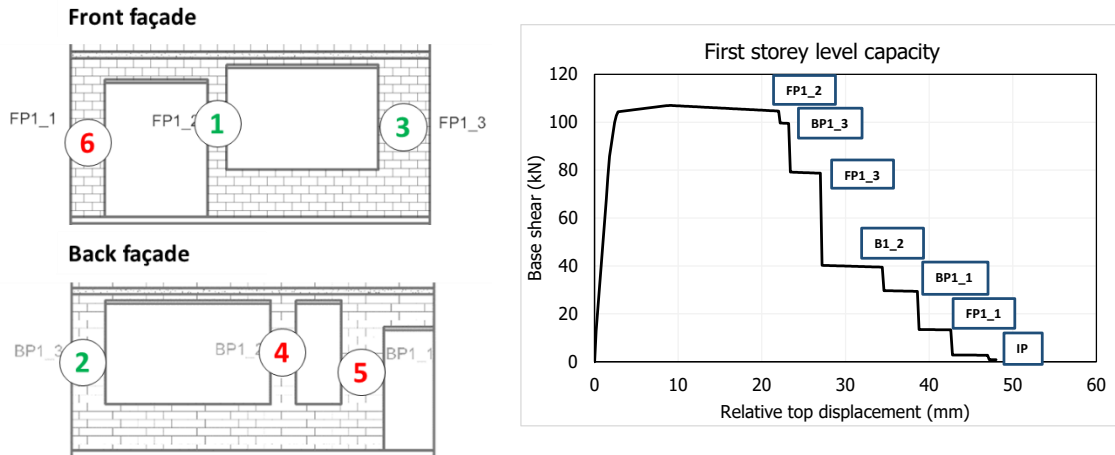

Figure 10. Sequence of NC collapse of the piers on the front and back façade for negative loading. The piers with a green number fail before the 50% drop, whereas those with a red number fail after that point.

The compliance of the building to NPR9998 is assessed for a specific site by comparing the bilinear capacity curve with the nonlinear ADRS demand. As shown in Figure 11, the building complies to NPR9998 as regards the global in-plane capacity, since the performance point can be find on the capacity curve for a displacement of 23.4 mm. At this displacement, the system has a ductility factor of 10.6, and the considered hysteretic damping is equal to 15%.

The spectrum which corresponds to a unity capacity over demand (C/D) ratio is defined by scaling the initial spectrum considered for the site-specific assessment. It should be noted that in principle this is not correct, since each location has several parameters which define the corresponding spectrum and these parameters do not change proportionally. However, the calculation provides a reasonable estimate of the maximum PGA

for which the building remains compliant to the NPR9998 recommendations. The scaled spectrum has a PGA of 0.171 g, as shown in Figure 12.
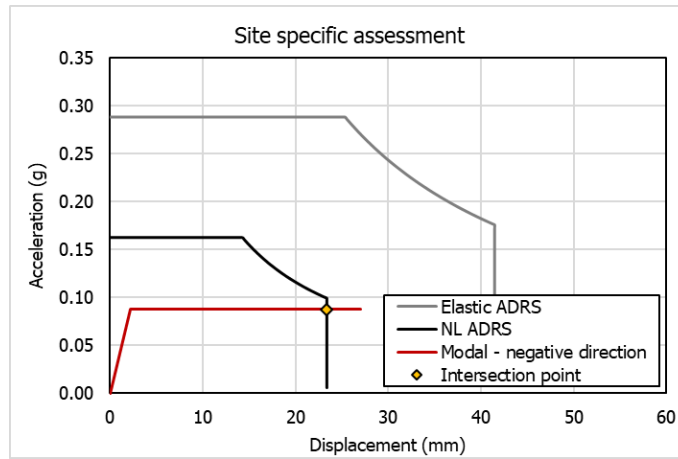

Figure 11. Site specific assessment for mode-proportional NLPO negative loading direction.
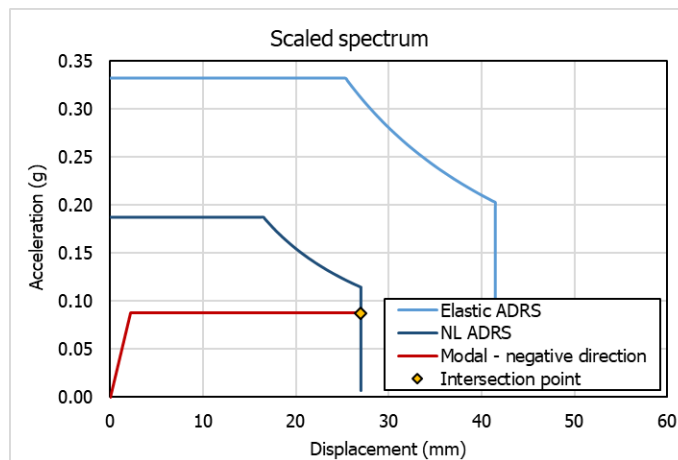

Figure 12. Scaled PGA assessment for mode-proportional NLPO negative loading direction.

4 Building C

The Building C is a terraced house characterised by the presence of bidirectional RC slabs at both first and second storey level. It is made of two building units with two appendices and an extra one-storey building. The two building units have an independent in-situ reinforced concrete diaphragm and can therefore be considered separately. The appendixes are assumed to be disconnected, and they are not modelled.

The discretization of the two facades is shown in Figure 13 and Figure 14 for the positive and negative loading, respectively. The internal walls are all modelled as cantilever piers, not connected to any other wall. As mentioned in Section 2, the spandrels are not modelled due to the presence of a bidirectional RC slab which constrain the rotations at the top of the piers.

The effective mass computed for the building is 69.2 t, assuming the first mode shape as linear.
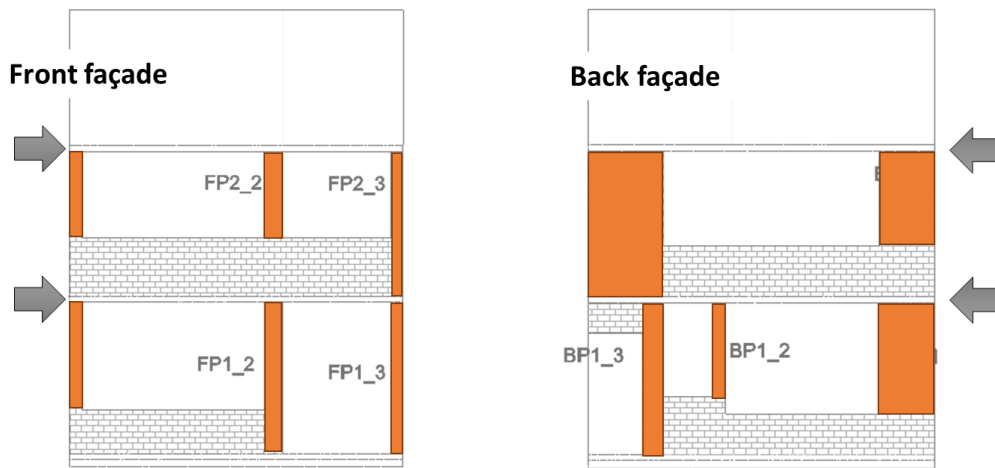
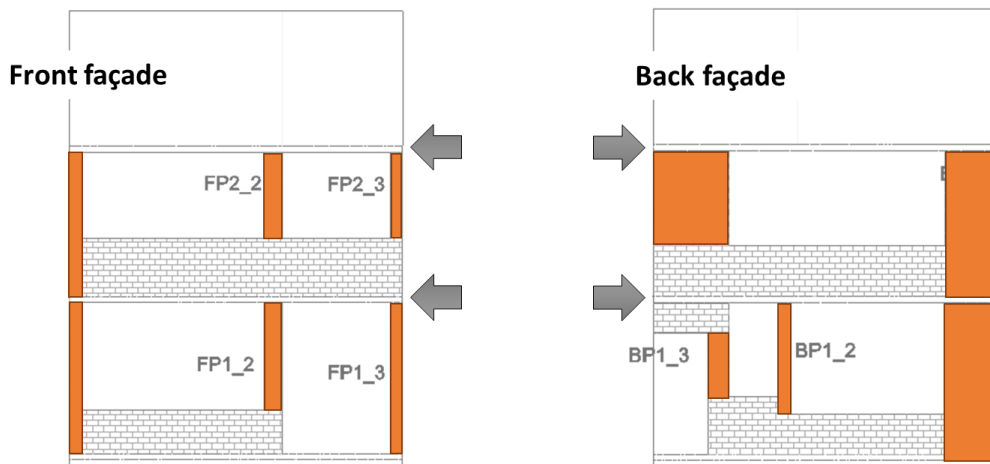Figure 13. Piers defined on the front and back façades of Building C for positive loading.

Figure 14. Piers defined on the front and back façades of Building C for negative loading.

4.1 Capacity of the structure

As described in section 2, the capacity is computed for each storey level and for both the mass-proportional and the mode-proportional lateral load distributions. The capacity curves obtained are shown in Figure 15 and

Figure 16 for the positive and negative loading direction, respectively. In both cases, the capacity of the ground storey level in terms of normalized accelerations is largely smaller than that of the first storey level. For this reason, a soft-storey mechanism at the ground-storey level is expected. Besides, the mode-proportional distribution of the lateral loads is governing for both the directions.
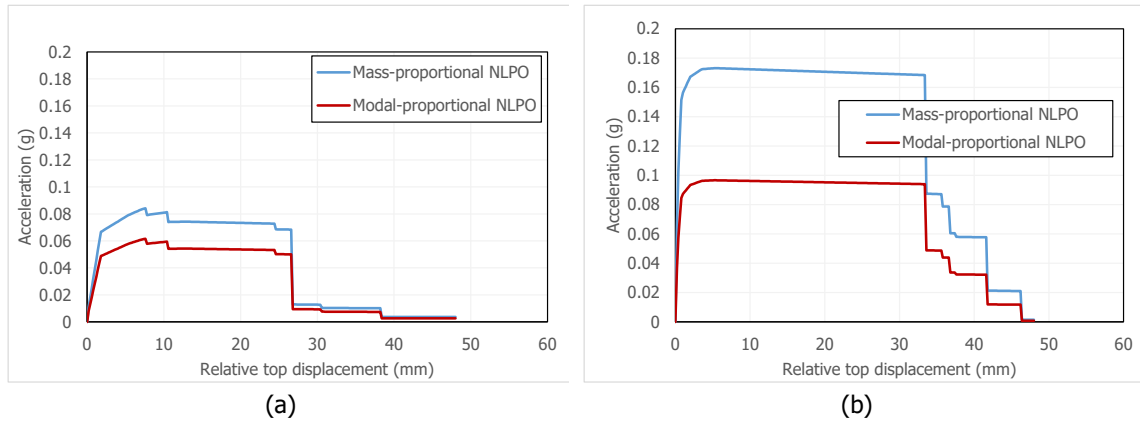

(a)   (b)

Figure 15. Capacity curve of the ground (a) and first (b) storey level for the positive loading direction.
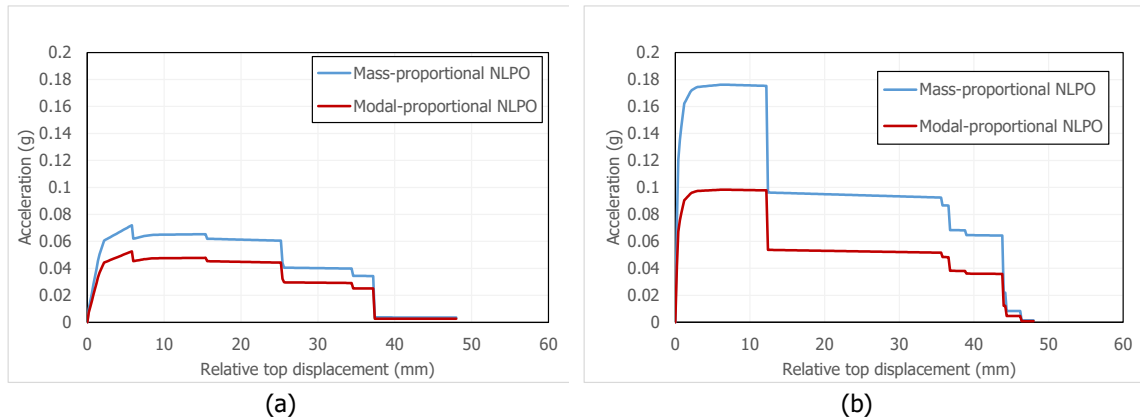

(a)   (b)

Figure 16. Capacity curve of the ground (a) and first (b) storey level for the negative loading direction.

The type of failure observed in each pier (either shear – as described in section G.9.2.2 of NPR9998 – or flexure – section G.9.2.3) is shown in Figure 17 and Figure 18 for positive and negative loading, respectively. The blue colour represents flexural failure and the green colour shear failure. It can be observed that flexure is governing for all the piers. Also all the internal non-loadbearing walls undergo flexural failure.

The overall behaviour of the structure can be therefore defined as 'ductile'; however, the limited length of the piers and the large axial loads limit the displacement capacity of the structure, also due to the second order effects. This is shown also by the equivalent bilinear curves derived for the structure and shown in Figure 19 (for the governing mode-proportional lateral load distribution). The relevant points of the curves are reported in Table 2.

The near collapse (NC) displacement is computed at the point corresponding to a 50% drop of the force capacity with respect to the peak load, since the sequence of failure of the piers does not show the complete failure of a façade before that the NC displacement is achieved, as shown in Figure 20 and Figure 21 for positive displacements and negative loading, respectively (it should be noted that the piers with a green number fail before the 50% drop, whereas those with a red number fail after that point).

The bilinear curve for positive displacements has a slightly larger capacity in terms of normalized acceleration, but a smaller displacement capacity. For this reason, the positive direction is the one considered for the assessment of the building.
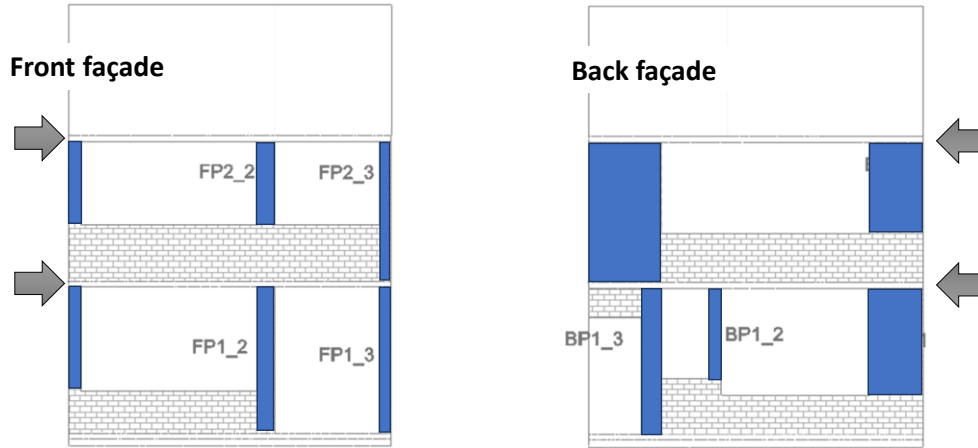
Figure 17. Failure of the piers of the front and back façades for positive loading. The blue colour represents a flexural failure and the green colour a shear failure.
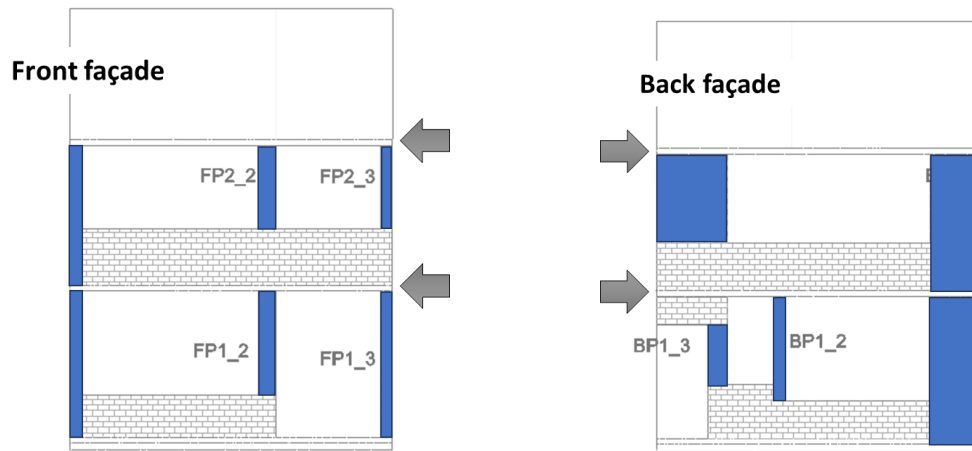

Figure 18. Failure of the piers of the front and back façades for negative loading. The blue colour represents a flexural failure and the green colour a shear failure.
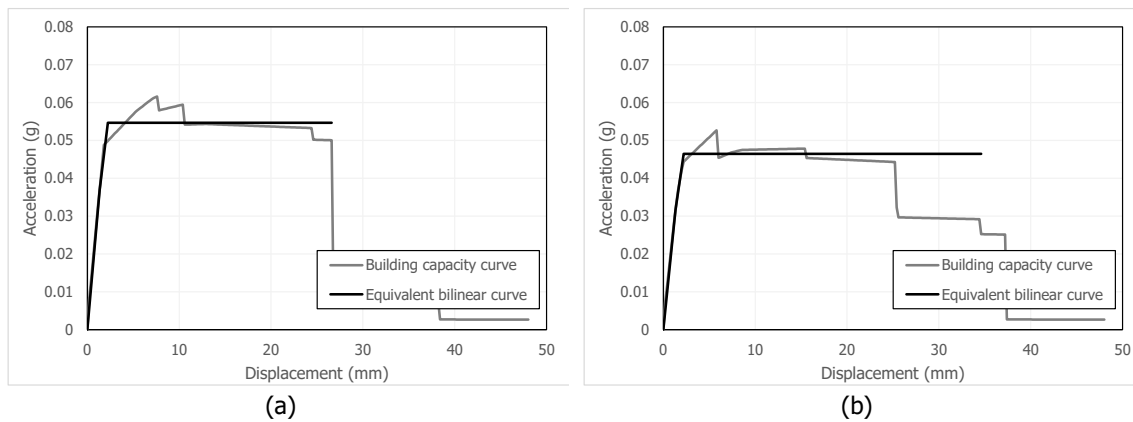

(a)　　　　　　　　　　　　　　　　　(b)

Figure 19. Equivalent bilinear capacity curve derived for the mode-proportional NLPO, for positive (a) and negative (b) loading direction.

Table 2. Relevant points of the equivalent bilinear curves.

	d_y (mm)	d_{NC} (mm)	a_{max} (g)
Positive loading	2.22	26.6	0.055
Negative loading	2.20	34.6	0.046

Figure 20. Sequence of NC collapse of the piers on the front and back façade for positive loading. The piers with a green number fail before the 50% drop, whereas those with a red number fail after that point.
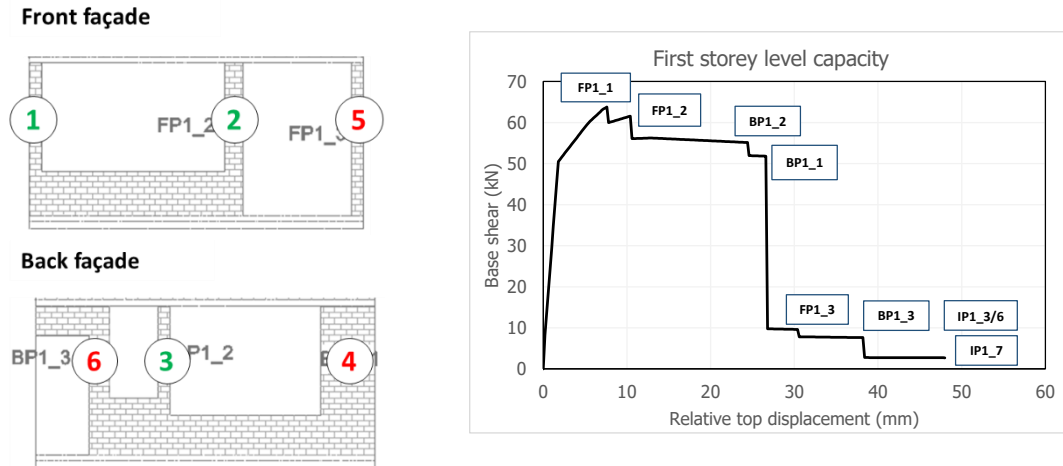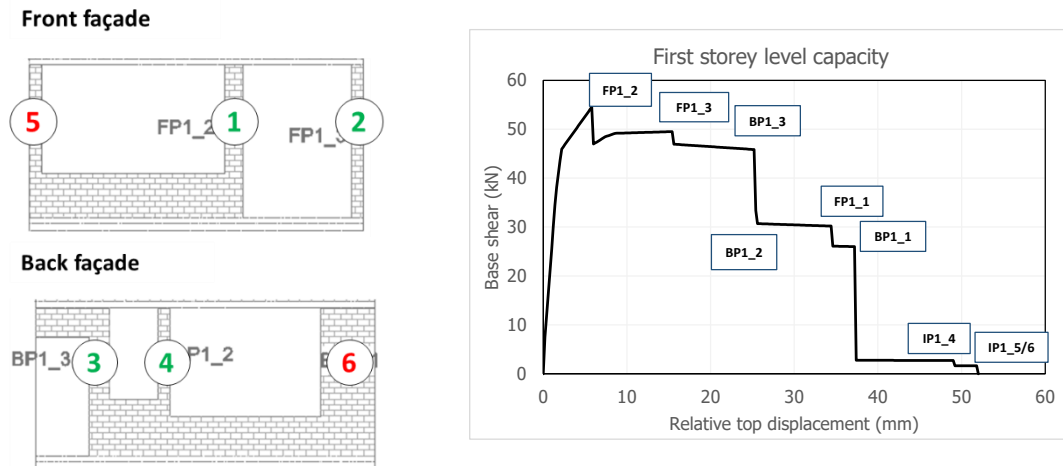

Figure 21. Sequence of NC collapse of the piers on the front and back façade for negative loading. The piers with a green number fail before the 50% drop, whereas those with a red number fail after that point.

The compliance of the building to NPR9998 is assessed for a specific site by comparing the bilinear capacity curve with the nonlinear ADRS demand. As shown in Figure 22, the building complies to NPR9998 as regards the global in-plane capacity, since the performance point can be find on the capacity curve for a displacement of 23.4 mm. At this displacement, the system has a ductility factor of 10.5, and the considered hysteretic damping is equal to 15%.

The spectrum which corresponds to a unity capacity over demand (C/D) ratio is defined by scaling the initial spectrum considered for the site-specific assessment. It should be noted that in principle this is not correct, since each location has several parameters which define the corresponding spectrum and these parameters do not change proportionally. However, the calculation provides a reasonable estimate of the maximum PGA

for which the building remains compliant to the NPR9998 recommendations. The scaled spectrum has a PGA of 0.200 g, as shown in Figure 23.
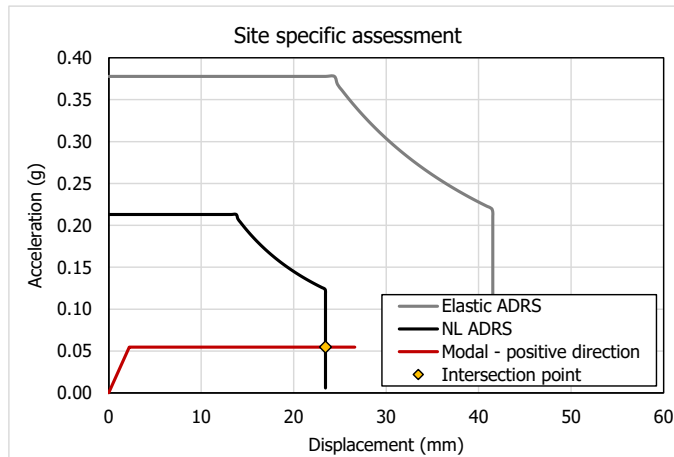

Figure 22. Site specific assessment for mode-proportional NLPO positive loading direction.
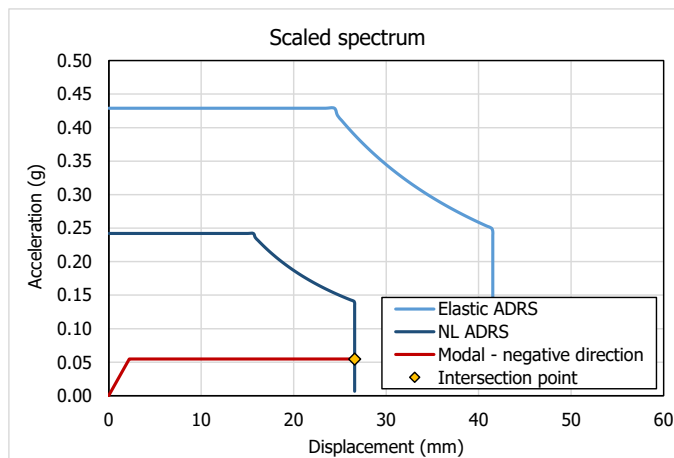

Figure 23. Scaled PGA assessment for mode-proportional NLPO positive loading direction.

5 Building D

Building D comprises of four building units with extra four annexes. The latter are connected only to the outer leaf of the house and for this reason they are not modelled. A cast in-situ reinforced concrete slab is present at both floor levels and acts as a rigid diaphragm across all four building units. However, for the sake of simplicity, only one building unit has been considered in the analysis.

The discretization of the two facades is shown in Figure 24 and Figure 25 for the positive and negative loading, respectively. The internal walls are all modelled as cantilever piers, not connected to any other wall. As mentioned in Section 2, the spandrels are not modelled due to the presence of a bidirectional RC slab which constrain the rotations at the top of the piers.

The effective mass computed for the building is 65.5 t, assuming the first mode shape as linear.
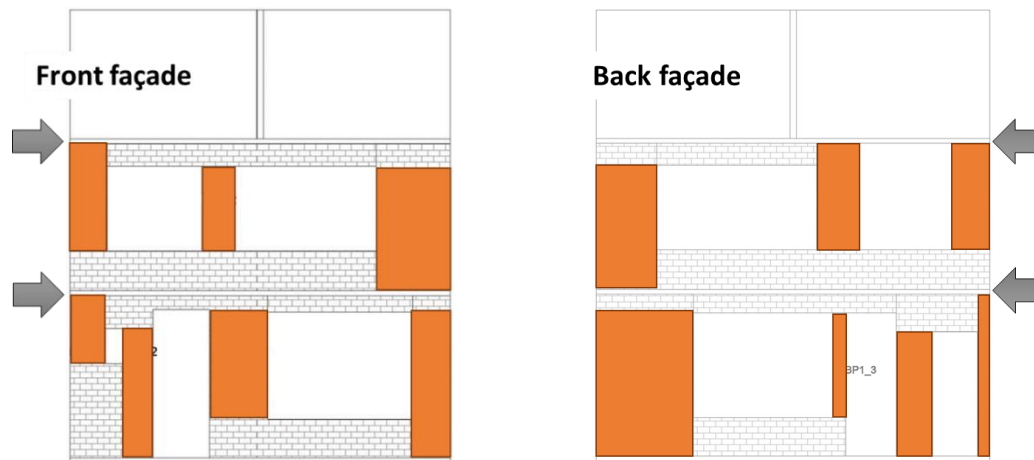

Figure 24. Piers defined on the front and back façades of Building D house for positive loading.
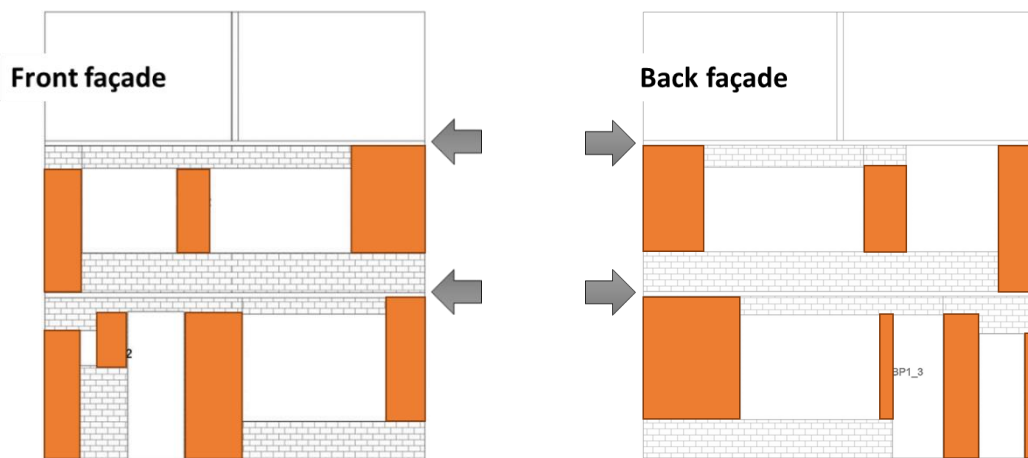
Figure 25. Piers defined on the front and back façades of Building D house for negative loading.

5.1 Capacity of the structure

As described in section 2, the capacity is computed for each storey level and for both the mass-proportional and the mode-proportional lateral load distributions. The capacity curves obtained are shown in Figure 26 and Figure 27 for the positive and negative loading direction, respectively. In both cases, the capacity of the first

storey level in terms of normalized accelerations is slightly smaller than that of the ground storey level. For this reason, a mechanism at the first-storey level is expected. However, given the limited difference the lower level may be also governing: it should be noted that this mechanism is less ductile, and its activation may lead to more critical performance for the vulnerability assessment (since this mainly depends on the displacement capacity of the structure). For this reason, it may be opportune to consider the assessment for both the possible failure mechanisms in addition to that presented in the following.

The mode-proportional distribution of the lateral loads is governing for both the directions.
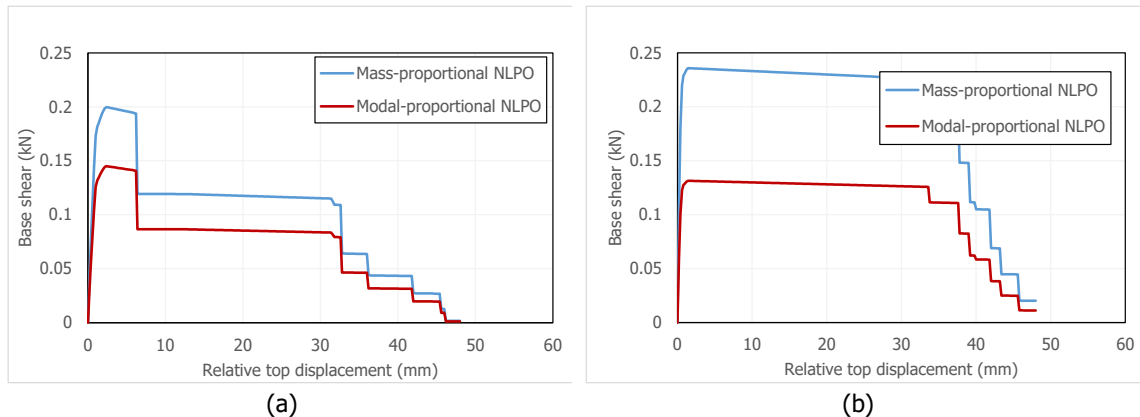

(a)   (b)

Figure 26. Capacity curve of the ground (a) and first (b) storey level for the positive loading direction.

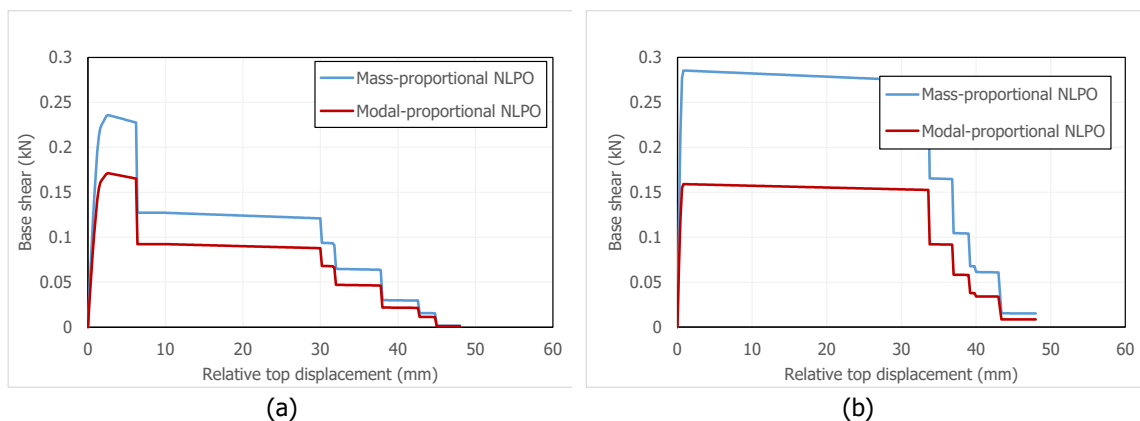(a)   (b)

Figure 27. Capacity curve of the ground (a) and first (b) storey level for the negative loading direction.

The type of failure observed in each pier (either shear – as described in section G.9.2.2 of NPR9998 – or flexure – section G.9.2.3) is shown in Figure 17 and Figure 18 for positive and negative loading, respectively. The blue colour represents flexural failure and the green colour shear failure. It can be observed that flexure is governing for all the piers except for a pier at the ground floor (which does not affect, hence, the most critical mechanism). All the internal non-loadbearing walls undergo flexural failure. The overall behaviour of the structure can be therefore defined as 'ductile'. This is shown also by the equivalent bilinear curves derived for the structure and shown in Figure 30 (for the governing mode-proportional lateral load distribution). The relevant points of the curves are reported in Table 2.

The near collapse (NC) displacement is computed at the point corresponding to a 50% drop of the force capacity with respect to the peak load, since the sequence of failure of the piers does not show the complete failure of a façade before that the NC displacement is achieved, as shown in Figure 31 and Figure 32 for positive displacements and negative loading, respectively (it should be noted that the piers with a green number fail before the 50% drop, whereas those with a red number fail after that point; the missing numbers correspond to internal walls).

The bilinear curve for positive displacements has a slightly smaller capacity in terms of normalized acceleration and the same displacement capacity than that for negative loading. For this reason, the positive direction is the one considered for the assessment of the building.
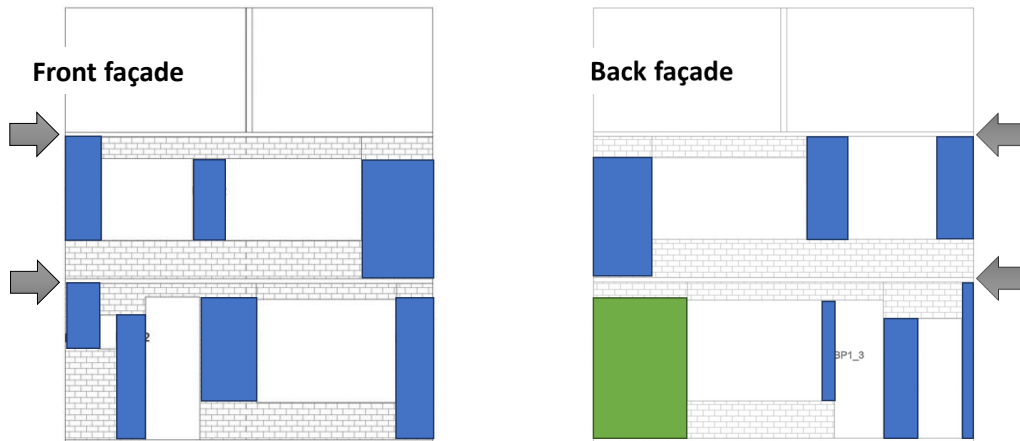

Figure 28. Failure of the piers of the front and back façades for positive loading. The blue colour represents a flexural failure and the green colour a shear failure.
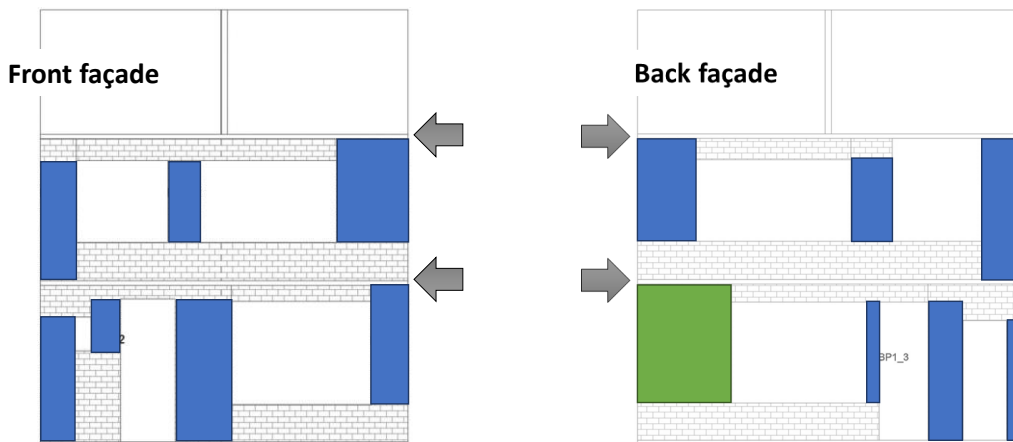

Figure 29. Failure of the piers of the front and back façades for negative loading. The blue colour represents a flexural failure and the green colour a shear failure.

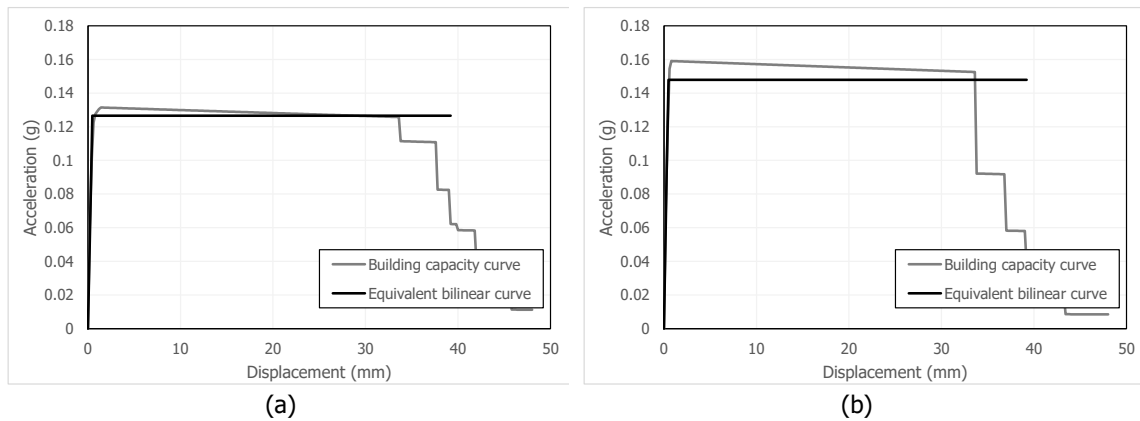(a)   (b)

Figure 30. Equivalent bilinear capacity curve derived for the mode-proportional NLPO, for positive (a) and negative (b) loading direction.

Table 3. Relevant points of the equivalent bilinear curves.

	d_y (mm)	d_{NC} (mm)	a_{max} (g)
Positive loading	0.49	39.2	0.127
Negative loading	0.30	39.2	0.148

Figure 31. Sequence of NC collapse of the piers on the front and back façade for positive loading. The piers with a green number fail before the 50% drop, whereas those with a red number fail after that point.
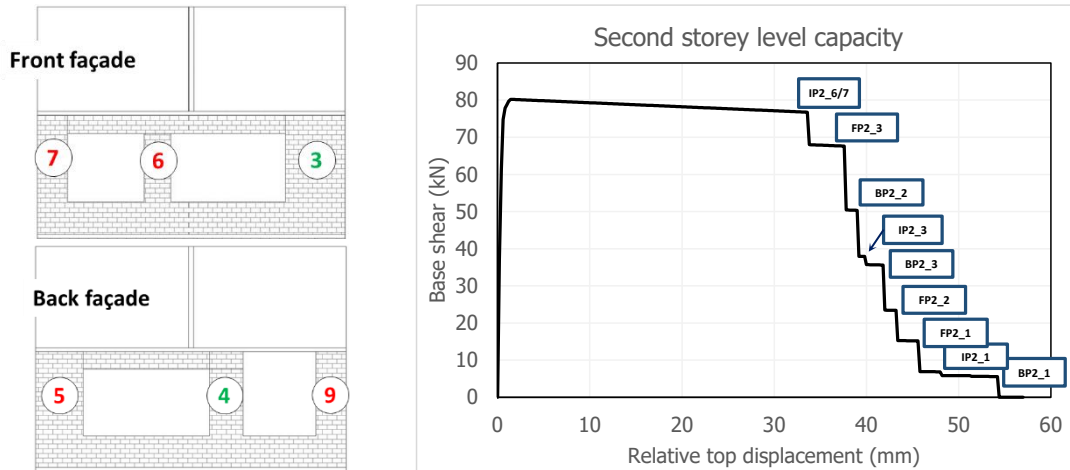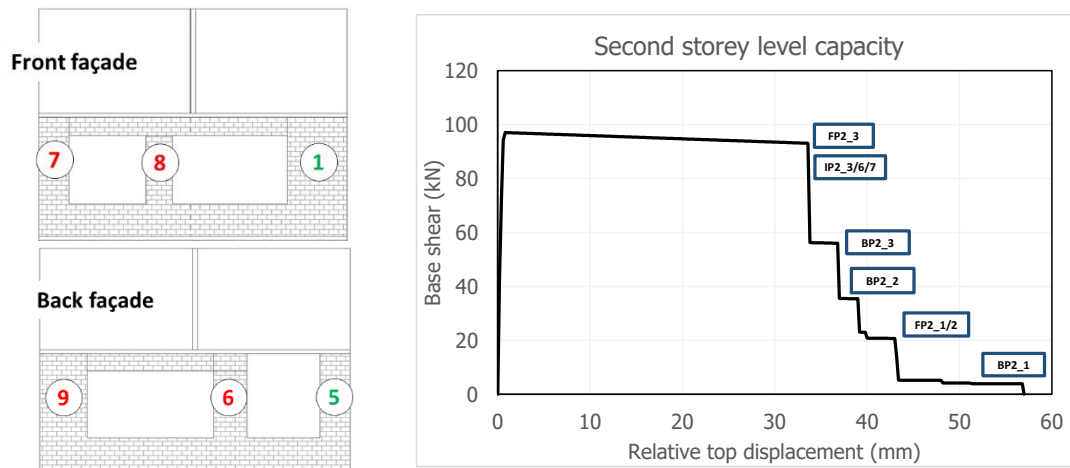

Figure 32. Sequence of NC collapse of the piers on the front and back façade for negative loading. The piers with a green number fail before the 50% drop, whereas those with a red number fail after that point.

The compliance of the building to NPR9998 is assessed for a specific site by comparing the bilinear capacity curve with the nonlinear ADRS demand. As shown in Figure 33, the building complies to NPR9998 as regards the global in-plane capacity, since the performance point can be find on the capacity curve for a displacement of 18.5 mm. At this displacement, the system has a ductility factor of 10.5, and the considered hysteretic damping is equal to 15%.

The spectrum which corresponds to a unity capacity/demand (C/D) ratio is defined by scaling the initial spectrum considered for the site-specific assessment. It should be noted that in principle this is not correct, since each location has several parameters which define the corresponding spectrum and these parameters do not change proportionally. However, the calculation provides a reasonable estimate of the maximum PGA

for which the building remains compliant to the NPR9998 recommendations. The scaled spectrum has a PGA of 0.248 g, as shown in Figure 34.
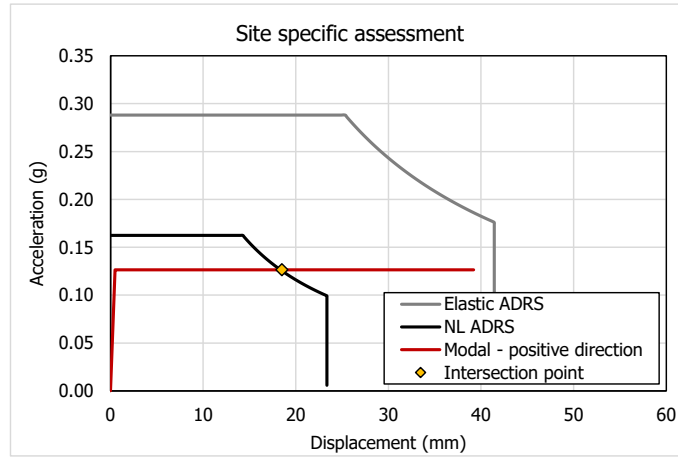

Figure 33. Site specific assessment for mode-proportional NLPO positive loading direction.
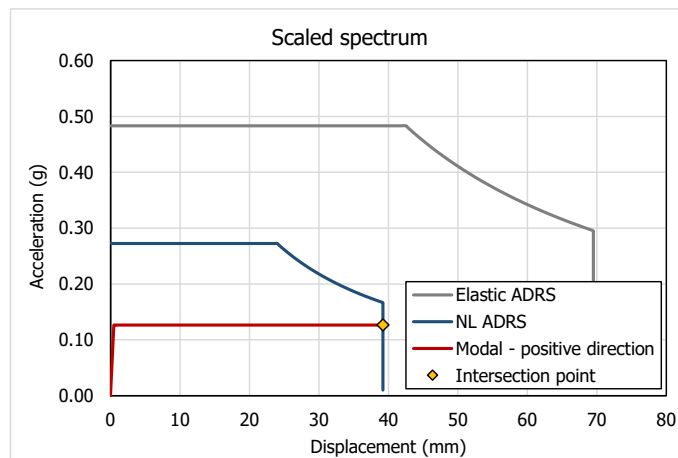

Figure 34. Scaled PGA assessment for mode-proportional NLPO positive loading direction.

6   Summary of the performance of the three buildings

Figure 35 shows the bilinear capacity curves, whereas Table 4 summarized the most relevant results obtained for the three investigated buildings.

All the three buildings show a ductile failure mechanism. Building B and Building C have similar performance in terms of displacement capacity, but Building B can reach larger accelerations. They both present a soft storey mechanism at the ground floor. Building D presents better performance compared to the other two buildings, as regards both the force and the displacement capacity. The capacity of the ground storey and of the first storey level is similar, although the latter is predicted to fail first.

The maximum PGA obtained for Building C is larger than for Building B. However, this depends by the original spectrum which has been amplified: in fact, since the two buildings have the same displacement capacity it is expected that they can withstand also a spectrum with the same PGA. At the most, the PGA of Building B should be higher given the larger force capacity of the building.

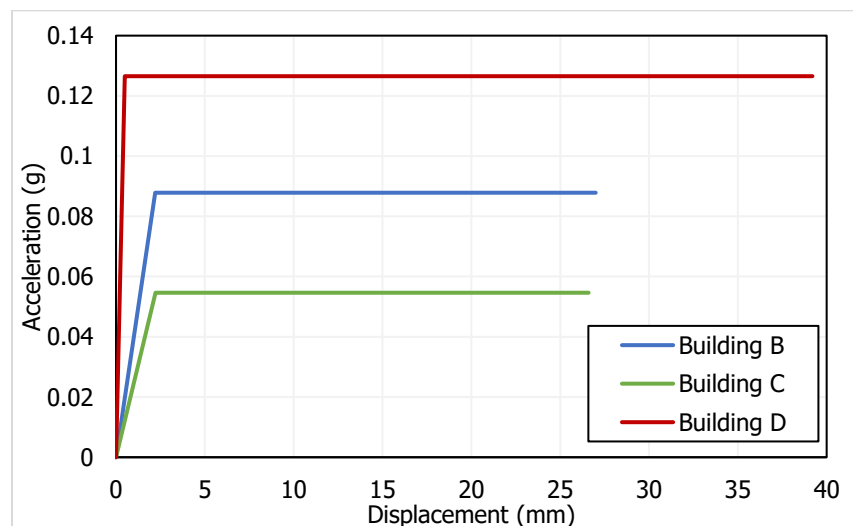The mode-proportional NLPO analysis is governing for all the buildings.

Figure 35. Bilinear capacity curves for the three studied buildings

Table 4. Summary of the main results of the SLaMA NLPO of the three buildings

Building	Governing storey level	Type of failure	Governing lateral load distribution	Governing direction	a_{max} (g)	d_{NC} (mm)	Site specific C/D	Max PGA
Building B	Ground storey	Ductile	Mode-proportional	Negative	0.088	27.0	1.16	0.171
Building C	Ground storey	Ductile	Mode-proportional	Positive	0.055	26.6	1.14	0.200
Building D	First storey	Ductile	Mode-proportional	Positive	0.127	39.2	1.68	0.248

Reference

[1] NEN (2018) - Assessment of the structural safety of buildings in case of erection, reconstruction, and disapproval - Induced earthquakes – Basis of design, actions and resistances. NPR9998:2018, NEN.

[2] NEN (2018) - Webtool NPR 9998: Bepaling van de seismische belasting. Available from URL: http://seismischekrachten.nen.nl/

[3] Yi, T., Moon, F. L., Leon, R. T., & Kahn, L. F. (2008). Flange effects on the nonlinear behaviour of URM piers. The Masonry Society Journal, 26(2), 31-42.